



Title	On the uniqueness of the approximate analytical solution of the surf-riding threshold in the IMO second generation intact stability criteria
Author(s)	Sakai, Masahiro; Umeda, Naoya
Citation	Journal of Marine Science and Technology. 2025
Version Type	VoR
URL	https://hdl.handle.net/11094/102739
rights	This article is licensed under a Creative Commons Attribution 4.0 International License.
Note	

The University of Osaka Institutional Knowledge Archive : OUKA

<https://ir.library.osaka-u.ac.jp/>

The University of Osaka



On the uniqueness of the approximate analytical solution of the surf-riding threshold in the IMO second generation intact stability criteria

Masahiro Sakai¹ · Naoya Umeda¹

Received: 16 July 2024 / Accepted: 3 July 2025
© The Author(s) 2025

Abstract

The International Maritime Organization developed the Second Generation Intact Stability Criteria (SGISC) with the objective of mitigating maritime incidents attributable to roll motion. Given that surf-riding precedes broaching, the SGISC uses vulnerability criteria for broaching based on surf-riding dynamics. The surf-riding threshold is derived by Melnikov's method in the level-2 vulnerability criterion. In this paper, the authors discuss the uniqueness of the approximate analytical solutions to be used as the surf-riding threshold in the SGISC, based on the relationship between Melnikov's analysis and its physical interpretation.

Keywords Surf-riding · Melnikov's method · IMO second generation intact stability criteria · Unique solution

1 Introduction

The International Maritime Organization (IMO) developed the Second Generation Intact Stability Criteria (SGISC) with the objective of mitigating maritime incidents attributable to roll motion. The interim guidelines for the SGISC were completed by the IMO's Subcommittee on Ship Design and Construction in 2020 [1] and are currently undergoing a trial period. The SGISC assesses five dynamic stability failure modes, including dead ship condition, excessive acceleration, pure loss of stability, parametric rolling, and surf-riding/broaching. Among these failure modes, broaching has been identified as a potential cause of sudden capsizing, particularly for smaller and faster vessels, as documented in real-world cases by Saunders [2] and Andrew [3]. Broaching occurs when a ship cannot maintain a straight course despite maximum steering efforts, with the resulting centrifugal force causing a severe heel moment. Given that surf-riding precedes broaching, the SGISC uses level-1 and level-2 vulnerability criteria for broaching based on surf-riding dynamics [1, 4]. In particular, the level-2 vulnerability

criterion employs a surf-riding threshold, beyond which the ship falls into surf-riding regardless of the initial conditions. Throughout this paper, unless explicitly stated otherwise, the term “surf-riding threshold” specifically refers to this condition. For further theoretical details on the vulnerability criteria, refer to [5, 6].

The study of a threshold of surf-riding could be considered to start with Grim's work [7], where he provided a physical description of the phenomenon. He argued that the surf-riding threshold can be defined as the condition in which a ship starts at an unstable equilibrium point with a speed equal to the wave speed, travels a full wavelength, and has once again reached a speed equal to the wave speed upon reaching the next unstable equilibrium point. Later, with the introduction of nonlinear dynamical systems theory into ship stability analysis, this surf-riding threshold was mathematically characterized as a heteroclinic bifurcation. Du Cane and Goodrich [8] realised surf-riding of a self-propelled ship model in a towing tank. Makov [9] substantiated Grim's argument by illustrating surf-riding phase planes and discovered that a self-propelled ship experiences surf-riding regardless of the initial condition with experimental validation once Grim's threshold is satisfied. Utilizing the surf-riding threshold is that a periodic attractor of an uncoupled surge model with linear thrust and resistance coincides with a separatrix loop, Kan [10] provided an analytical formula for estimating this threshold with a perturbation theory

✉ Masahiro Sakai
sakai@naoe.eng.osaka-u.ac.jp

¹ Graduate School of Engineering, The University of Osaka,
2-1 Yamadaoka, Suita, Osaka 565-0871, Japan

starting from the Hamiltonian system, which consists of only the inertia and wave exiting terms, assuming that the damping term as well as the difference between the ship nominal speed and wave celerity are small. As reconfirmed by Maki et al. [6], this method is known as the Melnikov analysis [11, 12]. However, because of the linear thrust and resistance the accuracy of the proposed formula is limited. Thus, he also provided an empirically modified formula as well. Spyrou [13] further pointed out the notion that the surf-riding threshold corresponds to a global bifurcation. Spyrou [14] provided an exact analytical solution for the heteroclinic bifurcation of an uncoupled surge model with quadratic calm-water resistance. Umeda et al. [15] used a numerical method to directly obtain the heteroclinic bifurcation point as the surf-riding threshold in regular following and stern quartering waves. Ananiev [16] analytically estimated the surf-riding threshold as the loss of stable periodic surge motion in place of the emergence of the heteroclinic connection.

Later on, Melnikov's method was implemented for estimating the surf-riding threshold in the SGISC. Following Kan's linear approach [10, 17], Spyrou [18] applied Melnikov's method to a surge model with cubic calm-water resistance. Furthermore, Maki et al. [19, 20] extended these studies by applying Melnikov's method to an uncoupled surge model with general polynomial calm-water resistances, determining the surf-riding thresholds, and validating these results through numerical bifurcation analysis and free-running model experiments. For further experimental validation of surf-riding estimates or the level-2 vulnerability criterion, refer to [21, 22]. Wu et al. [23] extended Melnikov's method to handle large damping and forcing effects, improving the prediction accuracy of surf-riding thresholds compared to the standard method, although losing a closed-form solution.

The IMO adopted the method using quintic calm-water resistance for the level-2 vulnerability criterion [1, 4], recommending the use of a numerical iteration method to determine the surf-riding threshold derived by Melnikov's method. However, this approach involves uncertainties regarding whether the numerical iteration yields a unique and convergent solution. Sakai et al. [24] remarked that the surf-riding threshold can instead be obtained as a solution to a quadratic equation when the propeller thrust coefficient is represented by a quadratic polynomial. Responding to their work, this quadratic equation approach was added to the explanatory notes to the SGISC [4], providing a way to eliminate the uncertainties associated with the numerical iteration method. However, since a quadratic equation could have two solutions, the uniqueness of the relevant solution should be discussed further. This study aims to prove the uniqueness of the approximate analytical solution derived using Melnikov's method, where the propeller thrust coefficient is expressed as a quadratic polynomial, and to examine

its physical interpretation within the SGISC framework. While a quadratic equation has two distinct real roots if the discriminant is positive, one repeated real root if the discriminant is zero, and no real roots if the discriminant is negative, only one physically meaningful surf-riding threshold should exist. Therefore, the quadratic equation determining the surf-riding threshold must always have a single positive real solution to be physically valid. The objective of this study is to demonstrate that this condition is invariably met under general conditions relevant to ship surf-riding, ensuring consistency with physical reality.

The initial results of the investigation presented in this paper were previously described by Sakai et al. [24]. In this paper, the results are presented more extensively, with more details, and also with new remarks.

2 Mathematical model of surf-riding and surf-riding threshold by Melnikov's method

In this section, the authors briefly explain the level-2 vulnerability criterion for broaching in the SGISC. The uncoupled surge equation used is

$$(m + m_x)\ddot{\xi}_G + [R(u) - T_e(u;n)] - X_w(\xi_G) = 0 \quad (1)$$

Here, m is the mass of the ship, m_x is the added mass in surge of the ship, ξ_G is the relative position of the ship centre of gravity from a wave trough where the wave propagating direction is set as positive, $R(u)$ is the calm-water resistance as a function of the ship instantaneous forward speed u , $T_e(u;n)$ is the effective propeller thrust as a function of u and number of revolutions of the propeller(s) n , and X_w is the wave-induced surge force. In this equation, the variation in thrust due to the wave particle velocity and higher-order terms, such as the added resistance in waves, are ignored.

When a ship surf-rides a wave at $\xi_G = \xi_{G,SR}$, the ship runs at the same speed as the wave celerity c_w , and the resistance, effective thrust and wave-induced surge force are balanced. In other words, the existence of n satisfying Eq. 2 is a necessary condition for surf-riding.

$$-R(c_w) + T_e(c_w;n) + X_w(\xi_{G,SR}) = 0 \quad (2)$$

Note that surf-riding could occur regardless of the initial conditions if n is in a certain range, and the boundaries of this range correspond to global bifurcation points, known as the heteroclinic bifurcation points. In the level-2 vulnerability criterion, the ship is considered vulnerable to broaching if n exceeds n_{cr} . Here, n_{cr} represents the lower value among the revolution numbers of the propeller(s) that correspond to the two heteroclinic bifurcation points. The schematic view

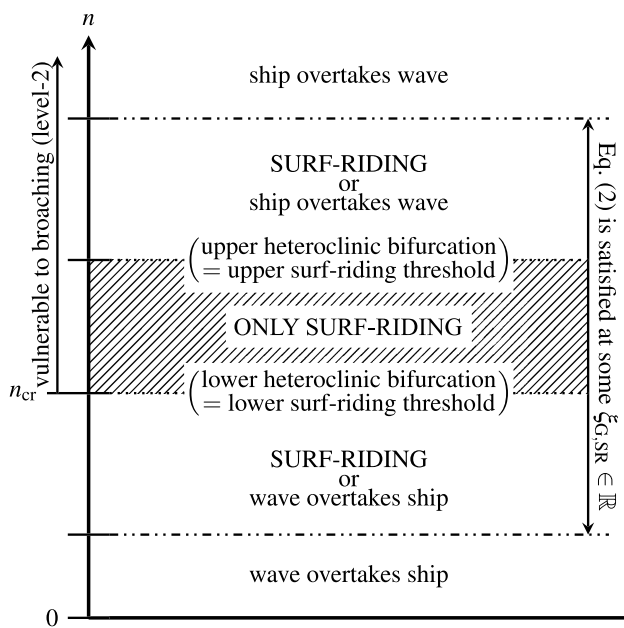


Fig. 1 Schematic view of bifurcations in Eq. 1 with respect to n and their relevance to the level-2 vulnerability criterion

of bifurcations in Eq. 1 with respect to n and their relevance to the level-2 vulnerability criterion are illustrated in Fig. 1.

Melnikov's method is used to obtain the heteroclinic bifurcation point, which is the surf-riding threshold. It is an approximate analytical method for obtaining homoclinic or heteroclinic orbits in nonlinear dynamical systems. Maki et al. [19] derived the equations of n_{cr} using Melnikov's method. They approximated $R(u)$ and $T_e(u; n)$ with N th-degree polynomials of u and J as

$$R(u) = \sum_{i=0}^N r_i u^i \quad (3)$$

$$J(u; n) = \frac{(1 - w_p)u}{nD} \quad (4)$$

$$K_T(J(u; n)) = \sum_{i=0}^N \kappa_i J(u; n)^i \quad (5)$$

$$T_e(u; n) = (1 - t_p) \rho n^2 D^4 K_T(J(u; n)) \\ = \sum_{i=0}^N \kappa_i (1 - t_p) (1 - w_p)^i \rho D^{4-i} n^{2-i} u^i \quad (6)$$

Here, w_p is the effective wake fraction, t_p is the thrust deduction coefficient, ρ is the density of the fluid, D is the propeller diameter, J is the advance coefficient and $K_T(J)$ is

the propeller thrust coefficient as a function of J . Here, u is calculated as

$$u = c_w + \dot{\xi}_G \quad (7)$$

Assuming

$$X_w \simeq -f \sin(k \xi_G) \quad (8)$$

Here, f is the amplitude of the wave-induced surge force, k is the wave number calculated as $\frac{2\pi}{\lambda}$, and λ is the wavelength. Substituting Eqs. 3 and 6 to 8 into Eq. 1 yields

$$(m + m_x) \ddot{\xi}_G + \sum_{i=1}^N \sum_{j=1}^i c_i(n) \binom{i}{j} c_w^{i-j} \xi_G^j \text{EMPTY}^j \\ = -R(c_w) + T_e(c_w; n) - f \sin(k \xi_G) \quad (9)$$

where

$$c_i(n) = -\frac{(1 - t_p)(1 - w_p)^i \rho \kappa_i}{n^{i-2} D^{i-4}} + r_i \quad (10)$$

Here, $\binom{i}{j}$ indicates the binomial coefficient. Putting

$$y = k \xi_G \quad (11)$$

$$\tau = \sqrt{\frac{fk}{m + m_x}} t \quad (12)$$

yields

$$\frac{d^2 y}{d\tau^2} + \sum_{i=1}^N \sum_{j=1}^i C_{ij}(n) \left(\frac{dy}{d\tau} \right)^j + \sin y = \frac{T_e(c_w; n) - R(c_w)}{f} \quad (13)$$

where

$$C_{ij}(n_{cr}) = c_i(n_{cr}) \cdot \frac{1}{fk^j} \binom{i}{j} \frac{(fk)^{\frac{j}{2}}}{(m + m_x)^{\frac{j}{2}}} c_w^{i-j} \quad (14)$$

The Hamilton part of Eq. 13 is

$$\frac{d^2 y}{d\tau^2} + \sin y = 0 \quad (15)$$

and the trajectory that connects $y = \pm\pi$ on the lower side of the vector field is

$$\frac{dy}{d\tau} = -2 \cos\left(\frac{y}{2}\right) \triangleq v \quad (16)$$

Maki et al. [19] obtained the Melnikov function $M(n)$ by approximating the heteroclinic orbit by the trajectory given by Eq. 16 as

$$M(n) \triangleq \int_{-\infty}^{\infty} v \left(\frac{T_e(c_w; n) - R(c_w)}{f} - \sum_{i=1}^N \sum_{j=1}^i C_{ij}(n) \left(\frac{dy}{d\tau} \right)^j \right) d\tau \quad (17)$$

Substituting Eq. 16 into Eq. 17 and changing variables yield

$$2\pi \frac{T_e(c_w; n_{cr}) - R(c_w)}{f} = \sum_{i=1}^N \sum_{j=1}^i C_{ij}(n_{cr}) \cdot (-2)^j I_j \quad (18)$$

where

$$I_j \triangleq \int_{-\pi}^{\pi} \cos^j \left(\frac{y}{2} \right) dy = 2\sqrt{\pi} \frac{\Gamma\left(\frac{j+1}{2}\right)}{\Gamma\left(\frac{j+2}{2}\right)} \quad (19)$$

Here, Γ indicates the Gamma function.

$R(u)$ and $K_T(J)$ are approximated by quintic and quadratic polynomials, respectively, in the level-2 vulnerability criterion. The calm-water resistance coefficient, normalised with the square of ship speed, covering the Froude number for the “last hump” can be represented by a cubic polynomial. The thrust coefficient can be modeled with a quadratic polynomial based on a blade element theory. Therefore, $N = 5$ and $\kappa_i = 0$ for $i = 3, 4, 5$.

3 Derivation of quadratic equation for the surf-riding threshold

As mentioned in Sect. 2, $K_T(J)$ is often approximated by a quadratic polynomial in the field of naval architecture, namely,

$$\kappa_i = 0 \quad (i \neq 0, 1, 2) \quad (20)$$

In the context of surf-riding, it is reasonable to assume $u, n \in \mathbb{R}_{\geq 0}$, and in this region, the values of κ_i are such that

$$\kappa_0 > 0 \quad (21)$$

$$\kappa_2 < 0 \quad (22)$$

κ_0 should be positive because K_T should be positive when $J = 0$, that is, $u = 0$ and $n > 0$. κ_2 should be negative because κ_2 should represent the K_T reduction when J is large enough. Then, Eq. 6 can be rewritten as

$$T_e(u; n) = \tau_0 n^2 + \tau_1 n u + \tau_2 u^2 \quad (23)$$

where

$$\tau_0 = \kappa_0 (1 - t_p) \rho D^4 > 0 \quad (24)$$

$$\tau_1 = \kappa_1 (1 - t_p) (1 - w_p) \rho D^3 \text{ EMPTY} \quad (25)$$

$$\tau_2 = \kappa_2 (1 - t_p) (1 - w_p)^2 \rho D^2 < 0 \quad (26)$$

Assuming $N > 2$, Eq. 10 becomes

$$c_i(n) = \begin{cases} -\tau_1 n + r_1 & (i = 1) \\ -\tau_2 + r_2 & (i = 2) \\ r_i & (i = 3, 4, \dots, N) \\ 0 & (i \neq 1, 2, \dots, N) \end{cases} \quad (27)$$

The right-hand side of Eq. 18 can be rewritten as

$$\begin{aligned} & \sum_{i=1}^N \sum_{j=1}^i C_{ij}(n_{cr}) \cdot (-2)^j I_j \\ &= 8 \frac{\tau_1 n_{cr} - r_1}{\sqrt{fk(m + m_x)}} \\ &+ \sum_{j=1}^2 (-\tau_2 + r_2) \frac{1}{fk^j} \binom{i}{j} \frac{(fk)^{\frac{j}{2}}}{(m + m_x)^{\frac{j}{2}}} c_w^{i-j} \cdot (-2)^j I_j \\ &+ \sum_{i=3}^N \sum_{j=1}^i r_i \frac{1}{fk^j} \binom{i}{j} \frac{(fk)^{\frac{j}{2}}}{(m + m_x)^{\frac{j}{2}}} c_w^{i-j} \cdot (-2)^j I_j \end{aligned} \quad (28)$$

As a result of assuming $K_T(J)$ is quadratic, the right-hand side of Eq. 18 becomes a 1st-degree polynomial of n_{cr} , and the left-hand side of Eq. 18 becomes a 2nd-degree polynomial of n_{cr} . Therefore, the surf-riding threshold can be estimated using a quadratic equation as

$$\begin{aligned} & 2\pi \frac{\tau_0}{f} n_{cr} \text{EMPTY}^2 + \left[2\pi \frac{\tau_1 c_w}{f} - 8 \frac{\tau_1}{\sqrt{fk(m + m_x)}} \right] n_{cr} \\ & - 2\pi \frac{R(c_w)}{f} + 8 \frac{r_1}{\sqrt{fk(m + m_x)}} \\ & - \sum_{j=1}^2 (-\tau_2 + r_2) \frac{1}{fk^j} \binom{i}{j} \frac{(fk)^{\frac{j}{2}}}{(m + m_x)^{\frac{j}{2}}} c_w^{i-j} \cdot (-2)^j I_j \\ & - \sum_{i=3}^N \sum_{j=1}^i r_i \frac{1}{fk^j} \binom{i}{j} \frac{(fk)^{\frac{j}{2}}}{(m + m_x)^{\frac{j}{2}}} c_w^{i-j} \cdot (-2)^j I_j = 0 \end{aligned} \quad (29)$$

Note that the above discussion in this section is independent of the degree of the polynomial of the calm-water resistance $R(u)$.

In the level-2 vulnerability criterion, the vulnerability to broaching is examined setting $N = 5$. Therefore, Eq. 29 can be rewritten as

$$2\pi \frac{T_e(c_w, n_{cr}) - R(c_w)}{f} + 8a_0 n_{cr} + 8a_1 - 4\pi a_2 + \frac{64}{3}a_3 - 12\pi a_4 + \frac{1024}{15}a_5 = 0 \quad (30)$$

where

$$a_0 = -\frac{\tau_1}{\sqrt{f k (m + m_x)}} \quad (31)$$

$$a_1 = \frac{r_1 + 2r_2 c_w + 3r_3 c_w EMPT Y^2 + 4r_4 c_w EMPT Y^3 + 5r_5 c_w EMPT Y^4 - 2\tau_2 c_w}{\sqrt{f k (m + m_x)}} \quad (32)$$

$$a_2 = \frac{r_2 + 3r_3 c_w + 6r_4 c_w EMPT Y^2 + 10r_5 c_w EMPT Y^3 - \tau_2}{k(m + m_x)} \quad (33)$$

$$a_3 = \frac{r_3 + 4r_4 c_w + 10r_5 c_w EMPT Y^2}{\sqrt{k^3 (m + m_x)^3}} \sqrt{f} \quad (34)$$

$$a_4 = \frac{r_4 + 5r_5 c_w}{k^2 (m + m_x)^2} f \quad (35)$$

$$a_5 = \frac{r_5}{\sqrt{k^5 (m + m_x)^5}} \sqrt{f^3} \quad (36)$$

Eq. 30 can be rewritten as

$$m_2 n_{cr} EMPT Y^2 + m_1 n_{cr} + m_0 = 0 \quad (37)$$

by putting

$$m_0 = 2\pi \frac{\tau_2 c_w EMPT Y^2 - R(c_w)}{f} + 8a_1 - 4\pi a_2 + \frac{64}{3}a_3 - 12\pi a_4 + \frac{1024}{15}a_5 \quad (38)$$

$$m_1 = 2\pi \frac{\tau_1 c_w}{f} + 8a_0 \quad (39)$$

$$m_2 = 2\pi \frac{\tau_0}{f} \quad (40)$$

4 Physical interpretation of Melnikov's method for surf-riding threshold

Substituting Eq. 7 into Eq. 1 yields

$$(m + m_x) \ddot{\xi}_G + [R(u) - T_e(u; n)] + f \sin(k \xi_G) = 0 \quad (41)$$

and this can be re-written as

$$\frac{1}{\sqrt{\frac{fk}{m+m_x}}} k \ddot{\xi}_G + \frac{R(u) - T_e(u; n)}{f} + \sin(k \xi_G) = 0 \quad (42)$$

Putting Eqs. 11 and 12 nondimensionalizes Eq. 42 as

$$\frac{d^2 y}{d\tau^2} + \sin y = \frac{T_e(u; n) - R(u)}{f} \quad (43)$$

Here, u is still used in Eq. 43 in order to make the following discussion clear. The Hamiltonian part of Eq. 43 is Eq. 15, and the trajectory that connects $y = \pm\pi$ on the lower side of the vector field is Eq. 16. Figure 2 shows the schematic view of the heteroclinic orbit of Eq. 43.

Here, $\mathbf{X}_0, \mathbf{X}_1 \in \mathbb{R}^2$ are saddle-type equilibria (unstable surf-riding), and Γ_0 , which connects \mathbf{X}_0 and \mathbf{X}_1 , is the heteroclinic orbit. The Melnikov function that is obtained by Maki et al. [19] (Eq. 17) is equivalent to

$$M(n) = \int_{-\infty}^{\infty} v \left(\frac{T_e(u; n) - R(u)}{f} \right) d\tau \quad (44)$$

This is because Eq. 17 is obtained by performing Taylor's expansion around $u = c_w$ applied to the integrand of Eq. 44 after polynomial approximation given in Eqs. 3 and 6. In this integral, the integration interval represents that the

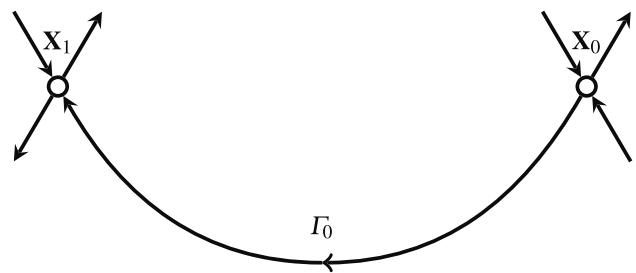


Fig. 2 Schematic view of heteroclinic orbit

heteroclinic orbit takes infinite time, and the integrand is proportional to the power generated by T_e and R . Under the surf-riding, the ship complies with Eq. 2. Substituting Eq. 8 into Eq. 2 yields

$$-R(c_w) + T_e(c_w; n) - f \sin(\xi_{G, SR}) = 0 \quad (45)$$

If n is enough large to satisfy Eq. 45, the unstable surf-riding \mathbf{X}_l (l is an integer) is

$$\mathbf{X}_l = \begin{pmatrix} \xi_{G, SR} \\ \dot{\xi}_{G, SR} \end{pmatrix} = \begin{pmatrix} \arcsin\left(\frac{T_e(c_w; n) - R(c_w)}{f}\right) - 2\pi l \\ 0 \end{pmatrix} \quad (46)$$

Since the potential energy due to $f \sin(k\xi_G)$ at the unstable equilibria is the same, the net work done by the calm-water resistance R and the effective propeller thrust T_e must be balanced along the heteroclinic orbit. This balance is formulated in Melnikov's method, where the surf-riding threshold is obtained as the critical propeller revolution number n_{cr} that satisfies this condition. Therefore, n_{cr} is derived as the solution of $M(n_{cr}) = 0$.

$$\int_{-\infty}^{\infty} v T_e(u; n_{cr}) d\tau = \int_{-\infty}^{\infty} v R(u) d\tau \quad (47)$$

Substituting Eq. 16 into Eq. 47, changing variables, and dividing the both-sides with -2π yield

$$\frac{1}{2\pi} \int_{-\pi}^{\pi} T_e(u; n_{cr}) dy = \frac{1}{2\pi} \int_{-\pi}^{\pi} R(u) dy \quad (48)$$

The ship instantaneous forward speed u used for the integral in Eq. 48 is defined by Eq. 7 and is transformed in the framework of Melnikov's method as

$$\begin{aligned} u &= c_w + \dot{\xi}_G \\ &= c_w + \sqrt{\frac{f}{k(m+m_x)}} \frac{dy}{d\tau} \\ &= c_w - 2\sqrt{\frac{f}{k(m+m_x)}} \cos\left(\frac{y}{2}\right) \end{aligned} \quad (49)$$

Based on the linear deep-water dispersion relation, c_w is

$$c_w = \sqrt{\frac{g}{k}} \quad (50)$$

Here, g is the gravitational acceleration.

5 Uniqueness of the surf-riding threshold

This section demonstrates the uniqueness of the surf-riding threshold in the framework of Melnikov's method. First, the authors start with the quadratic $K_T(J)$, which is adopted

in the level-2 vulnerability criterion for broaching in the SGISC. Substituting Eq. 23 into Eq. 48 yields

$$\frac{1}{2\pi} \int_{-\pi}^{\pi} (\tau_0 n_{cr} EMPTY^2 + \tau_1 u n_{cr} + \tau_2 u^2) dy = \frac{1}{2\pi} \int_{-\pi}^{\pi} R(u) dy \quad (51)$$

The left-hand side is the quadratic function with n_{cr} . Since the following definite integrals with respect to y are calculated as

$$\frac{1}{2\pi} \int_{-\pi}^{\pi} dy = 1 \quad (52)$$

$$\frac{1}{2\pi} \int_{-\pi}^{\pi} u dy = c_w - \frac{4}{\pi} \sqrt{\frac{f}{k(m+m_x)}} \triangleq \mathbb{E}[u] \quad (53)$$

$$\begin{aligned} \frac{1}{2\pi} \int_{-\pi}^{\pi} u^2 dy &= c_w EMPTY^2 - \frac{8}{\pi} c_w \sqrt{\frac{f}{k(m+m_x)}} + 2 \frac{f}{k(m+m_x)} \\ &\triangleq \mathbb{E}[u^2] > 0 \end{aligned} \quad (54)$$

Equation (51) is rewritten as

$$\begin{aligned} \tau_0 n_{cr} EMPTY^2 + \tau_1 \mathbb{E}[u] n_{cr} + \tau_2 \mathbb{E}[u^2] &= \frac{1}{2\pi} \int_{-\pi}^{\pi} R(u) dy \\ \Leftrightarrow \tau_0 \left(n_{cr} - \frac{-\tau_1 \mathbb{E}[u]}{2\tau_0} \right)^2 - \tau_0 \left\{ \frac{(\tau_1 \mathbb{E}[u])^2}{4\tau_0 EMPTY^2} + \frac{-\tau_2 \mathbb{E}[u^2]}{\tau_0} \right\} \\ &= \frac{1}{2\pi} \int_{-\pi}^{\pi} R(u) dy \end{aligned} \quad (55)$$

Since τ_0 is positive as shown in Eq. 24, and since τ_2 is negative as shown in Eq. 26, the left-hand side is a convex downward quadratic function that is negative when n_{cr} is zero. The schematic view of the solution of Eq. 55 is shown in Fig. 3 as the crossing points of the quadratic function (the left-hand side of Eq. 55) and the straight line (the right-hand side of Eq. 55). Obviously, Eq. 55 has two distinct real roots, one positive and the other negative if

$$\frac{1}{2\pi} \int_{-\pi}^{\pi} R(u) dy > \tau_2 \mathbb{E}[u^2] \quad (56)$$

However, when n_{cr} is negative and u is positive, that is, adverse rotation of the propeller with the ship moving forward, the effective thrust of the propellers becomes negative and the K_T for $n \in \mathbb{R}_{\geq 0}$ is ineffective. Therefore, Eq. 55 always has a unique real n_{cr} regardless of the value of τ_1 .

In the level-2 vulnerability criterion, the surf-riding threshold n_{cr} can be derived from Eq. 37 and is given by

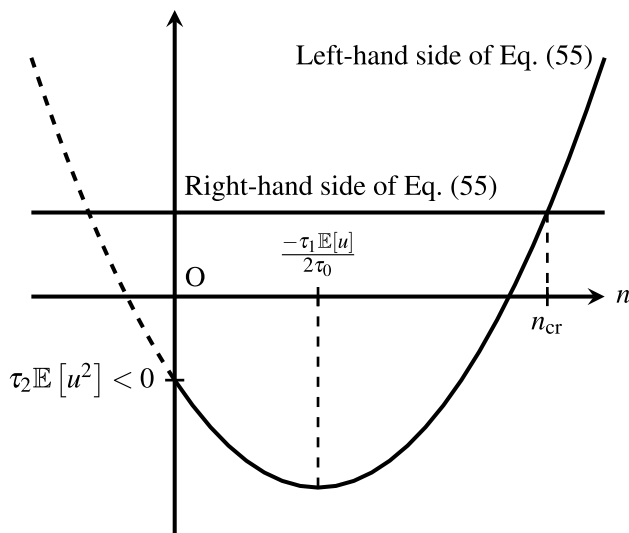


Fig. 3 Schematic view of the unique real solution of Eq. 55

$$n_{cr} = \frac{-m_1 + \sqrt{m_1^2 - 4m_0m_2}}{2m_2} \quad (57)$$

In the above discussion, it was demonstrated that the surf-riding threshold can be uniquely determined if the K_T is approximated under the condition of $n > 0$ and Eq. 56.

Further discussion of the equivalent wave condition under which the unique surf-riding threshold is given is provided in the appendix, and it is confirmed that Eq. 56 is satisfied in most waves.

6 Physical interpretation of the uniqueness of the surf-riding threshold

The relationship between T_e and $R(u)$, as stated in Eq. 48, is used to discuss the physical interpretation of the unique surf-riding threshold. In the context of surf-riding, it is reasonable to assume $u, n \in \mathbb{R}_{\geq 0}$. Under these conditions, T_e can be assumed to have the following properties.

1. T_e increases monotonically with n .
2. When $n = 0$, T_e has a negative finite value.

From the Sect. 5, the definite integral for the resistance on the right-hand side of Eq. 48 is constant with n . From the first point, the definite integral on the left-hand side of Eq. 48 increases monotonically with respect to n . The second point corresponds to the fact that the propeller generates a negative finite thrust when $u > 0$ and $n = 0$. Therefore, Eq. 48 always has a unique positive solution. The schematic

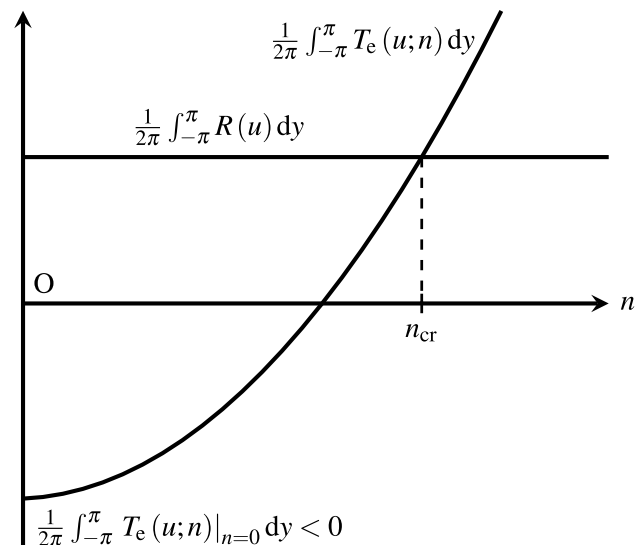


Fig. 4 Schematic view of the unique real solution of Eq. 48

view is shown in Fig. 4. Although $\frac{1}{2\pi} \int_{-\pi}^{\pi} T_e(u; n) dy$ does not always increase monotonically with small n in Fig. 3, this is simply due to the quadratic fitting of K_T with respect to J .

7 Conclusions

The authors discussed the uniqueness of the approximate analytical solution of the surf-riding threshold in the SGISC. The authors interpreted Melnikov's method in physical terms, viewing it as a balance between the work done by the effective thrust and resistance, and found that

1. the surf-riding threshold n_{cr} is obtained as the solution of a quadratic equation when K_T is expressed as a quadratic function of J as adopted in SGISC, which has two distinct real roots, one positive and the other negative;
2. the positive root is the unique surf-riding threshold if the right-hand side of Eq. 55 is positive;
3. in most of waves, the right-hand side of Eq. 55 is positive; and
4. the above does not depend on the approximation of the calm-water resistance R .

Appendix (Limiting Wave Steepness)

The unique surf-riding threshold is given when Eq. 56 is satisfied under Eq. 49 in the framework of Melnikov's method. Since the right-hand side of Eq. 56 is negative,

$$\int_{-\pi}^{\pi} R(u) dy > 0 \quad (58)$$

can be considered as the sufficient condition of Eq. 56. It is obvious that Eq. 58 is satisfied when $u > 0$ along the heteroclinic orbit because $R(u) > 0$ for all $u > 0$. From Eq. 49, The minimum value for u along the heteroclinic orbit occurs when

$$\cos\left(\frac{y}{2}\right) = 1 \quad (59)$$

This provides the condition

$$u > c_w - 2\sqrt{\frac{f}{k(m + m_x)}} \quad (60)$$

Rearranging this inequality for f using Eq. 50 results in

$$f < \frac{1}{4}(m + m_x)g \quad (61)$$

In steep waves where the inequality in Eq. 61 no longer holds, $u < 0$ occurs at some point on the heteroclinic orbit. Since $R(u) < 0$ for all $u < 0$, Eq. 58 is roughly equivalent to the mean ship speed on the heteroclinic orbit $\mathbb{E}[u]$ being positive. Rearranging $\mathbb{E}[u]$ for f using Eq. 50 results in

$$f < \frac{\pi^2}{16}(m + m_x)g \quad (62)$$

Let f_{R0} be defined as the amplitude of the wave-induced surge force that satisfies the following equation:

$$\int_{-\pi}^{\pi} R(u) dy = 0 \quad (63)$$

In reality, the calm-water resistance would be larger for $u < 0$ than for $u > 0$, so f_{R0} is considered to satisfy the following inequality:

$$\frac{1}{4}(m + m_x)g < f_{R0} < \frac{\pi^2}{16}(m + m_x)g \quad (64)$$

In the following discussion, the authors investigate the limiting wave steepness at which Eq. 58 is satisfied, which means that the sufficient condition for the uniqueness of the approximate analytical solution derived using Melnikov's method is met. This examination is based on Eq. 64, which provides the basis for determining the constraints on the wave-induced surge force. In the SGISC, the wave-induced surge force is calculated as the Froude–Krylov force. Therefore, its amplitude is calculated as

$$\begin{aligned} f &= \mu \cdot \rho g k \frac{H}{2} \sqrt{F_c EMPTY^2 + F_s EMPTY^2} \\ &= \mu \cdot \pi \rho g \frac{H}{\lambda} \sqrt{F_c EMPTY^2 + F_s EMPTY^2} \end{aligned} \quad (65)$$

where

$$F_c = \int S(x) \sin(kx) e^{-k \frac{d(x)}{2}} dx \quad (66)$$

$$F_s = \int S(x) \cos(kx) e^{-k \frac{d(x)}{2}} dx \quad (67)$$

$$m = \rho \int S(x) dx \quad (68)$$

Here, μ is the correction factor due to the diffraction effect, H is the wave height, x is the body-fixed coordinate system along the longitudinal direction ($x = 0$ indicates the midship), S is the area of the submerged portion at x and d is the draught at x . In the vulnerability criterion of the SGISC, the diffraction effect on the wave-induced surge force is neglected and is simply considered as $\mu = 1$. For operational guidance, the explanatory notes to the SGISC suggest numerical estimation of μ or the use of experimental correction factor [4, 22] as

$$\mu = \begin{cases} 1.46C_b - 0.05 & (C_m < 0.86) \\ (5.76 - 5.00C_m)C_b - 0.05 & (0.86 \geq C_m \geq 0.94) \\ 1.06C_b - 0.05 & (C_m > 0.94) \end{cases} \quad (69)$$

In simple terms, the value is almost $\mu = 0.7$ for the operational guidance.

An upper bound on f is considered with maximised wave slope acting on each submerged section as

$$\begin{aligned} f &< \mu \cdot \pi \rho g \frac{H}{\lambda} \int S(x) \cdot 1 \cdot 1 dx \\ &= \mu \cdot \pi \frac{H}{\lambda} mg \end{aligned} \quad (70)$$

Since $m_x \simeq 0.1m$, Eq. 70 can be rewritten as

$$f < \mu \cdot \frac{4\pi}{1.1} \frac{H}{\lambda} \cdot \frac{1}{4}(m + m_x)g \quad (71)$$

$$f < \mu \cdot \frac{16}{1.1\pi} \frac{H}{\lambda} \cdot \frac{\pi^2}{16}(m + m_x)g \quad (72)$$

As a result, Eqs. 61 and 62 is almost equivalent to the following wave condition

Table 1 Principal particulars and coefficients for calm-water resistance and effective propeller thrust of the 34.5m-long fishing vessel

Item	Value	Unit
Length between perpendiculars	34.5	m
Breadth	7.6	m
Draught	2.65	m
Trim	0.30	m
LCB (aft from the midship)	1.31	m
Block coefficient	0.597	
Service speed in Fn	0.40	
D	2.60	m
t_p	0.142	
w_p	0.156	
m_x/m	0.0667	
r_0	0	-
r_1	-4273.53	N s/m
r_2	7491.11	N s ² /m ²
r_3	-2668.12	N s ³ /m ³
r_4	408.20	N s ⁴ /m ⁴
r_5	-17.005	N s ⁵ /m ⁵
κ_0	0.2244	
κ_1	-0.2283	
κ_2	-0.1373	

Table 2 $S(x)$ and $d(x)$ of the 34.5m-long fishing vessel

x [m]	$S(x)$ [m ²]	$d(x)$ [m]
-21.65	0.00E+00	0
-20.55	1.85E+00	0.448703
-19.45	2.61E+00	0.539137
-18.35	3.28E+00	0.629572
-17.25	3.88E+00	0.715006
-15.53	5.40E+00	1.275049
-13.8	7.82E+00	3.255005
-12.075	1.04E+01	3.175004
-10.35	1.28E+01	3.105004
-6.9	1.61E+01	2.955002
-3.45	1.76E+01	2.800001
0	1.71E+01	2.65
3.45	1.58E+01	2.499999
6.9	1.38E+01	2.354998
10.35	1.04E+01	2.199996
12.075	8.00E+00	2.134996
13.8	5.24E+00	2.044995
15.525	2.86E+00	1.959995
17.25	1.17E+00	1.794994

$$\mu \cdot \frac{4\pi}{1.1} \frac{H}{\lambda} < 1$$

$$\Rightarrow \begin{cases} \frac{H}{\lambda} < \frac{1}{11.4} & (\mu = 1, \text{vulnerability criterion}) \\ \frac{H}{\lambda} < \frac{1}{8.00} & (\mu = 0.7, \text{operational guidance}) \end{cases} \quad (73)$$

$$\mu \cdot \frac{16}{1.1\pi} \frac{H}{\lambda} < 1$$

$$\Rightarrow \begin{cases} \frac{H}{\lambda} < \frac{1}{4.63} & (\mu = 1, \text{vulnerability criterion}) \\ \frac{H}{\lambda} < \frac{1}{3.24} & (\mu = 0.7, \text{operational guidance}) \end{cases} \quad (74)$$

Therefore, the wave condition for $\left(\frac{H}{\lambda}\right)_{R0}$ where Eq. 63 is satisfied is

$$\begin{cases} \frac{1}{11.4} < \left(\frac{H}{\lambda}\right)_{R0} < \frac{1}{4.63} & (\mu = 1, \text{vulnerability criterion}) \\ \frac{1}{8.00} < \left(\frac{H}{\lambda}\right)_{R0} < \frac{1}{3.24} & (\mu = 0.7, \text{operational guidance}) \end{cases} \quad (75)$$

In the vulnerability criterion, the maximum wave steepness is $0.15 \approx 1/6.67$. Therefore, there is the possibility that $u < 0$. However, Eq. 56 is usually satisfied.

Appendix (Sample Calculations)

Sample calculations were conducted using a 34.5m-long fishing vessel. The necessary data for the calculation were provided in Sect. 6, “Example of assessment of ship vulnerability to surf-riding/broaching,” in Appendix 2 of the explanatory notes to the SGISC [4] (Tables 1 and 2). Here, LCB is the longitudinal position of the centre of buoyancy. In the level-2 vulnerability criterion for broaching in the SGISC, Eq. 65 is calculated by using the discretized form of Eqs. (66) and (67) with coefficients shown in Table 2.

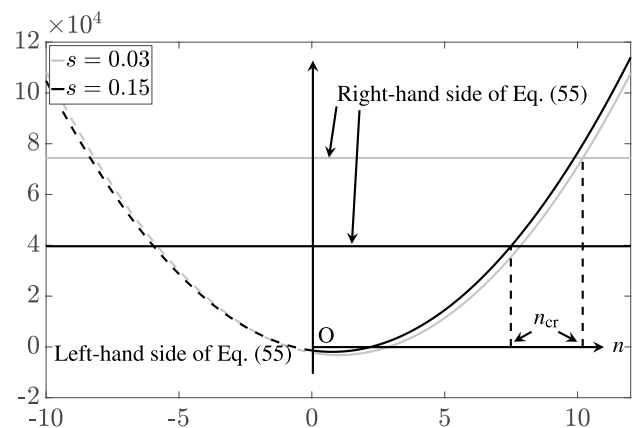


Fig. 5 Numerical examples indicating the unique real solution of Eq. 48 where s represents the wave steepness

The calculation results corresponding to Fig. 3 are presented in Fig. 5 for the cases of the wavelength to a ship length ratio of 1.0 and the wave steepnesses of 0.03 and 0.15. It is clearly observed that the left-hand side of Eq. 55 does not change significantly with respect to the wave steepness, while the decrease on the right-hand side of Eq. 55 mainly causes the surf-riding threshold to shift to the lower side of the propeller revolution number.

Acknowledgements The authors express great appreciation to Prof. Atsuo Maki of The University of Osaka for constructive suggestions and discussions. This study was supported by a Grant-in-Aid for Scientific Research from the Japan Society for the Promotion of Science (JSPS KAKENHI Grant JP21K14362).

Funding Open Access funding provided by The University of Osaka.

Data Availability The datasets generated and/or analysed during the current study are available from the corresponding author, M.S., upon reasonable request.

Declarations

Conflict of interest The authors declare that they have no Conflict of interest.

Open Access This article is licensed under a Creative Commons Attribution 4.0 International License, which permits use, sharing, adaptation, distribution and reproduction in any medium or format, as long as you give appropriate credit to the original author(s) and the source, provide a link to the Creative Commons licence, and indicate if changes were made. The images or other third party material in this article are included in the article's Creative Commons licence, unless indicated otherwise in a credit line to the material. If material is not included in the article's Creative Commons licence and your intended use is not permitted by statutory regulation or exceeds the permitted use, you will need to obtain permission directly from the copyright holder. To view a copy of this licence, visit <http://creativecommons.org/licenses/by/4.0/>.

References

1. IMO. MSC.1-Circ. 1627 - interim guidelines on the second generation intact stability criteria (2020)
2. Saunders H.E (1957) in *Hydrodynamics in Ship Design*, pp. 819–865
3. Andrew J.W (2012) The report of the commission of inquiry into the sinking of Rabaul Queen
4. IMO. MSC.1-Circ. 1652 - explanatory notes to the interim guidelines on second generation intact stability criteria (2022)
5. Umeda N, Yamamura S (2010) Designing new generation intact stability criteria on broaching associated with surf-riding. in *Proceedings of the 11th International Ship Stability Workshop, Wageningen*, pp. 17–25
6. Maki A, Sakai M, Ueta T (2024) Review of the analytical prediction method of surf-riding threshold in following sea, and its relation to IMO Second-Generation intact stability criteria. *Non-linear Theory Appl IEICE* 15(3):588
7. Grim O (1951) Das schiff von achtern auflaufender see, jahrbuch der schiffbautechnischen gesellschaft. *Jahrbuch der Schiffbautechnischen Gesellschaft* 45:264
8. DuCane P, Goodrich G.J (1961) The following sea, broaching and surging, *Royal Institution of Naval Architects Transactions*
9. Makov Y (1969) Some results of theoretical analysis of surf-riding in following seas, *Trans. Krylov Society, "Maneuverability and Seakeeping of Ships"* 126, 124
10. Kan M (1990) A guideline to avoid the dangerous surf-riding. in *Proceedings of the 4th international conference on stability of ships and ocean vehicles*, pp. 90–97
11. Melnikov VK (1963) On the stability of a center for time-periodic perturbations. *Trudy moskovskogo matematicheskogo obshchestva* 12:3
12. Holmes PJ (1980) Averaging and chaotic motions in forced oscillations. *SIAM J Appl Math* 38(1):65
13. Spyrou KJ (1996) Dynamic instability in quartering seas: the behavior of a ship during broaching. *J Ship Res* 40(01):46
14. Spyrou K.J (2001) Exact analytical solutions for asymmetric surging and surf-riding. in *Proceedings of 5th International Workshop "Stability and Operational Safety of Ships"*, pp. 4.4.1–4.4.3
15. Umeda N, Hori M, Hashimoto H (2007) Theoretical prediction of broaching in the light of local and global bifurcation analyses. *Int Shipbuild Prog* 54:269
16. Ananiev D.M (1966) On surf-riding in following seas, *T Krylov Soc* pp. 169–176
17. Kan M (1989) Surging of large amplitude and surf-riding of ships in following seas (part 3 phase plane analysis). in *Japan Society of Naval Architects and Ocean Engineers*, pp. 267–276
18. Spyrou KJ (2006) Asymmetric surging of ships in following seas and its repercussions for safety. *Nonlinear Dyn* 43(1–2):149
19. Maki A, Umeda N, Renilson M, Ueta T (2010) Analytical formulae for predicting the surf-riding threshold for a ship in following seas. *J Mar Sci Technol* 15(3):218
20. Maki A, Umeda N, Renilson M, Ueta T (2014) Analytical methods to predict the surf-riding threshold and the wave-blocking threshold in astern seas. *J Mar Sci Technol* 19(4):415
21. Yamamura S, Umeda N, Maki A, Sano H (2009) Numerical study towards Physics-Based criteria for avoiding broaching and capsizing in following/ quartering waves. in *Conference Proceedings of The Japan Society of Naval Architects and Ocean Engineers*, vol. 9K, pp. 109–112
22. Ito Y, Umeda N, Kubo H (2014) Hydrodynamic aspects on vulnerability criteria for surf-riding of ships, *J. Teknol.* 66(2)
23. Wu W, Spyrou KJ, McCue LS (2010) Improved prediction of the threshold of surf-riding of a ship in steep following seas. *Ocean Eng* 37(13):1103
24. Sakai M, Maki A, Murakami T, Umeda N (2017) Analytical solution of critical speed for Surf-Riding in the light of melnikov analysis. in *Conference Proceedings of the Japan Society of Naval Architects and Ocean Engineers*, vol. 24 (The Japan Society of Naval Architects and Ocean Engineers), vol. 24, pp. 311–314

Publisher's Note Springer Nature remains neutral with regard to jurisdictional claims in published maps and institutional affiliations.